ACCOUNTS of chemical research

Article

pubs.acs.org/accounts

Microfluidic Technology: Uncovering the Mechanisms of Nanocrystal Nucleation and Growth

Ioannis Lignos,[†,‡] Richard Maceiczyk,[†] and Andrew J. deMello*,[†]

[†]Institute for Chemical and Bioengineering, Department of Chemistry and Applied Biosciences, ETH Zurich, Vladimir-Prelog-Weg 1, Zurich 8093, Switzerland

Downloaded via ETH ZURICH on January 11, 2019 at 14:42:02 (UTC).
See https://pubs.acs.org/sharingguidelines for options on how to legitimately share published articles.

CONSPECTUS: The controlled and reproducible formation of colloidal semiconductor nanocrystals (or quantum dots) is of central importance in nanoscale science and technology. The tunable size- and shape-dependent properties of such materials make them ideal candidates for the development of efficient and low-cost displays, solar cells, light-emitting devices, and catalysts. The formidable difficulties associated with the macroscale preparation of semiconductor nanocrystals (possessing bespoke optical and chemical properties) result from the fact that underlying reaction mechanisms are complex and that the reactive environment is difficult to control. Automated microfluidic reactors coupled with monitoring systems and optimization algorithms aim to elucidate complex reaction mechanisms that govern both nucleation and growth of nanocrystals. Such platforms are ideally suited for the efficient optimization of reaction parameters, assuring the reproducible synthesis of nanocrystals with user-defined properties.

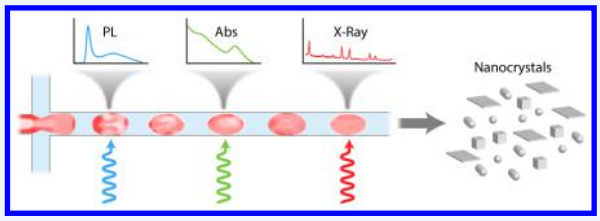

This Account aims to inform the nanomaterials community about how microfluidic technologies can supplement flask experimentation for the ensemble investigation of formation mechanisms and design of semiconductor nanocrystals. We present selected studies outlining the preparation of quantum dots using microfluidic systems with integrated analytics. Such microfluidic reaction systems leverage the ability to extract real-time information regarding optical, structural, and compositional characteristics of quantum dots during nucleation and growth stages.

The Account further highlights our recent research activities focused on the development and application of droplet-based microfluidics with integrated optical detection systems for the efficient and rapid screening of reaction conditions and a better understanding of the mechanisms of quantum dot synthesis. We describe the features and operation of fully automated microfluidic reactors and their subsequent application to high-throughput parametric screening of metal chalcogenides (CdSe, PbS, PbSe, CdSeTe), ternary and core/shell heavy metal-free quantum dots ($CuInS_2$, $CuInS_2$/ZnS), and all-inorganic perovskite nanocrystals ($CsPbX_3$, X = Cl, Br, I) syntheses. Critically, concurrent absorption and photoluminescence measurements on millisecond to second time scales allow the extraction of basic parameters governing nanocrystal formation. Moreover, experimental data obtained from such microfluidic platforms can be directly supported by theoretical models of nucleation and growth. To this end, we also describe the use of metamodeling algorithms able to accurately predict optimized conditions of CdSe synthesis using a minimal number of sample parameters.

Importantly, we discuss future challenges that must be addressed before microfluidic technologies are in a position to be widely adopted for the on-demand formation of nanocrystals. From a technology perspective, these challenges include the development of novel engineering platforms for the formation of complex architectures, the integration of monitoring systems able to harvest photophysical and structural information, the incorporation of continuous purification systems, and the application of optimization algorithms to multicomponent quantum dot systems.

1. INTRODUCTION

Recent years have seen considerable interest in the development of wet-chemical methods for the synthesis of colloidal semiconductor nanocrystals (NCs) or quantum dots (QDs), resulting in novel pathways for the control of NC size, shape, composition, and structure.[1−4] Such control is critical for the application of NCs in catalysis,[5] biological sensing and nanomedicine,[6] optoelectronics,[7] photovoltaics, and single photon sources.[7,8] Unfortunately, benchtop synthetic protocols are enunciated empirically since reaction mechanisms are poorly understood.[1,9] Conversely, microfluidic reactors (processing fluids within environments having internal dimensions on a scale of micrometers) are able to reassess standard synthetic approaches, while providing a unique environment for elucidating reaction kinetics.[10,11]

Over the past decade, microfluidic technology has been at the forefront of key developments in molecular and NC synthesis.[10,11] However, despite significant benefits, including rapid heat and mass transfer and the ability to precisely control reaction parameters,[10,11] microfluidic reactors have yet to be widely embraced by the nanomaterials community. This is primarily due to a lack of appreciation of the operational simplicity and fundamental advantages of microfluidic systems. Herein we review and discuss the use of microfluidic reactors to

Received: February 14, 2017
Published: May 3, 2017

 © 2017 American Chemical Society

DOI: 10.1021/acs.accounts.7b00088
Acc. Chem. Res. 2017, 50, 1248−1257

unveil the mechanisms of NC nucleation and growth and guide the efficient design of colloidal NCs. Moreover, we highlight issues that challenge the use of microfluidics in the production of novel nanomaterials and provide an outlook on developments in the short-to-medium term.

2. MICROFLUIDIC EXPERIMENTATION

Flow-based microfluidics can be categorized as continuous or segmented flow microfludics (Figure 1a).[10,11] Put simply, the reaction mixture can travel through the system either as a continuous stream or compartmentalized within femtoliter to nanoliter segments separated by an immiscible carrier fluid. Continuous flows are simple to establish and directly scalable, but their parabolic velocity profile across the channel cross-section together with unencumbered molecule/wall interactions leads to residence time distributions and subsequently poor control over particle size distributions.[10] Segmented flow reactors add operational complexity but immediately overcome the primary limitations of continuous flow reactors by isolating the reaction mixture and removing residence time distributions.[10] Importantly, both flow regimes can be realized in a variety of formats, including chip-based systems (fabricated from polymers, glass, or silicon) and capillary-based reactors. The choice of the material and format (Figure 1b,c) follows experimental needs and constraints.[10]

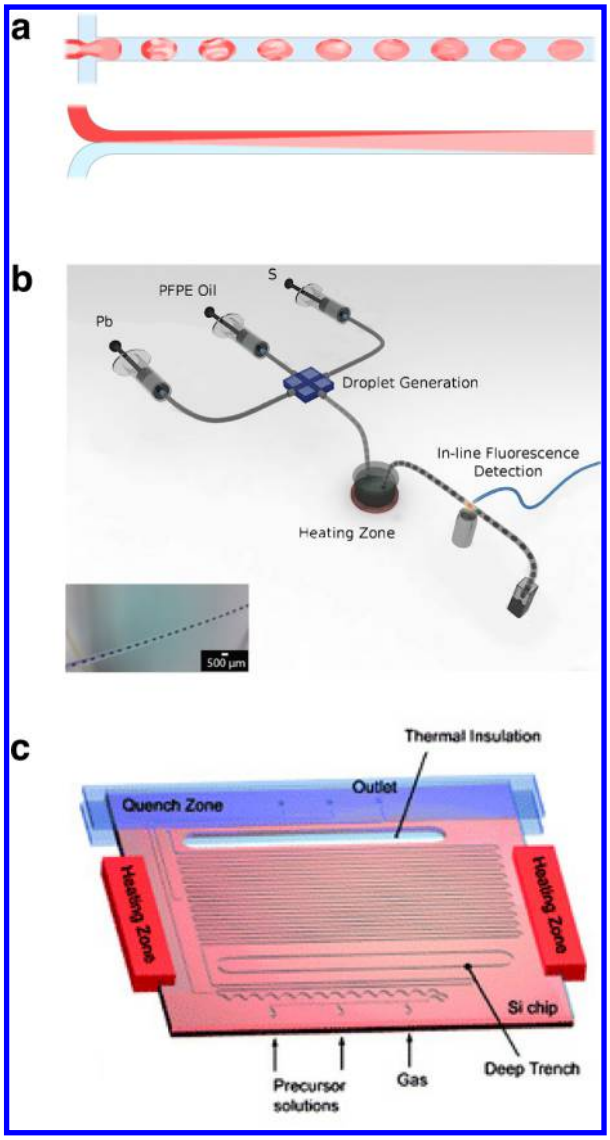

Figure 1. (a) Droplet-based and continuous flow formats in microfluidic channels. (b) A capillary-based reactor with integrated near-infrared detector for the formation of PbS and PbSe QDs. Inset: Image of droplets containing PbS QDs. Reprinted with permission from ref 12. Copyright 2014 American Chemical Society. (c) Silicon-based reactor with two heating zones the synthesis of QDs and reaction quenching. Reprinted with permission from ref 13. Copyright 2005 John Wiley and Sons.

The analysis of NCs using postsynthetic analytical methods is well-established and provides thorough characterization of the products. That said, "off-line" techniques are time-consuming and ill-suited to elucidate reaction pathways, as well as the influence of reaction parameters on reaction rates and yields.[14] Additionally, routinely performed purification after the synthesis often leads to a loss of structural and physicochemical information through alteration of both surface environment and particle−ligand interactions.[1] In contrast, microfluidic reactors with integrated detectors are well-suited for the rapid extraction of chemical information (Figure 1a), engendering a superior design of material properties and providing detailed insights into nucleation and growth processes.

3. MECHANISMS OF QUANTUM DOT NUCLEATION AND GROWTH

We now briefly discuss theoretical treatments of nucleation and growth, with a focus on models based on classical nucleation theory (CNT), in which nucleation proceeds via a single energy barrier.[9,15] Analytical theories[16−18] based on the work of Becker and Döring[19] and LaMer and Dinegar[20] often fail to give quantitative predictions due to the major assumptions and simplifications they incorporate.[15] Accordingly, many contemporary studies have revisited CNT and subjected it to a more precise numerical treatment with minimal analytical approximations. For example, Talapin et al.[21] studied the evolution of an ensemble of NCs through Monte Carlo simulations based on a single-particle growth law. The authors found that the first order approximation of the Gibbs−Thomson relation in LSW (Lifshitz−Slyozov−Wagner) theory fails to capture the dynamics of real NC populations and leads to an overestimated dispersion of the stationary particle size distribution. Additionally, such a theory is successful in relating the degree of initial supersaturation to the duration of focusing, as shown in Figure 2. Critically, the transferral of theoretical findings to the synthesis of CdSe NCs has since resulted in improvements in achievable product dispersity.[24] The stochastic nature of Monte Carlo simulations, however, prevents the identification of deterministic factors, which would provide further theoretical insight and improvements to synthetic protocols.[25] In a recent study, Robb and Privman[26] reformulated the classic treatment by LaMer to allow for quantitative numerical calculations, while assuming instant thermalization of subcritical nuclei and diffusion limited growth of nuclei above the critical radius.

In related studies, Mantzaris[25] used population balance equations (PBEs) to model the development of a seeded distribution of NCs based on a generalized single-particle growth law. The model recovered the analytical results of LSW-theory and provided quantitative insight on how diffusion and reaction influence the final size distribution. In agreement with the results of Rogach et al.,[24] he showed that the initial excess of monomer determines the extent of the reduction of the particle distribution during focusing. Additionally, results

DOI: 10.1021/acs.accounts.7b00088
Acc. Chem. Res. 2017, 50, 1248−1257

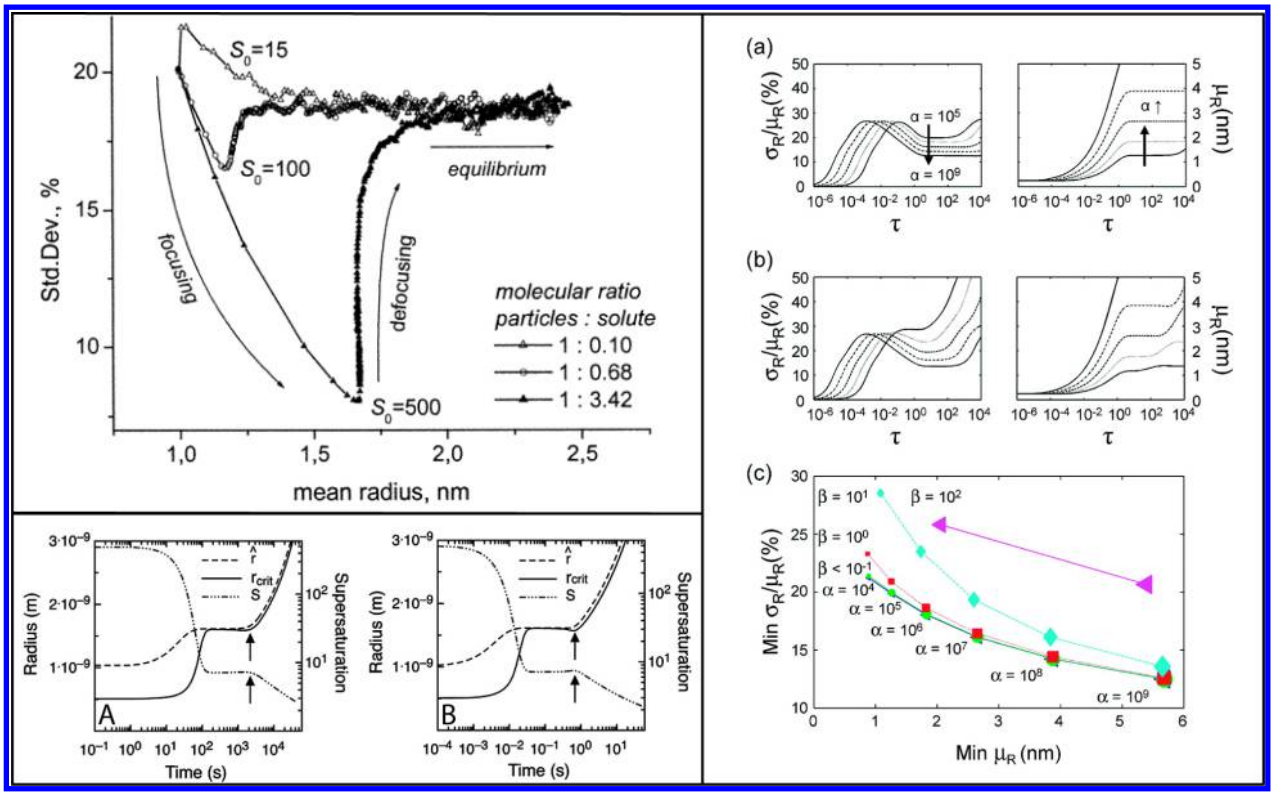

Figure 2. (top left) Dependence of the particle size distribution on the mean particle size for different initial oversaturations of monomer as obtained from Monte Carlo simulations. Reprinted with permission from ref 21. Copyright 2001 American Chemical Society. (bottom left) Temporal dynamics of the critical radius, r_{crit}, mean radius, $\hat{r}$, and supersaturation, S, for reaction (A) and diffusion-limited (B) growth calculated using a PBE model. Reprinted with permission from ref 22. Copyright 2009 American Chemical Society. (right) Evolution of the mean cluster radius computed and the percent radial distribution at order of magnitude increments of scaled growth rate parameter, α, ranging from 105 to 109 for (a) $\beta = 10^{-1}$ and (b) $\beta = 10^{1}$. (c) Minimum attained percent in the radial size distribution and the corresponding mean radial size at different values of the scaled growth and dissociation rate parameters α and β, respectively. Reprinted with permission from ref 23. Copyright 2009 American Chemical Society.

suggest that it is possible to extend focusing via continuous supplementation of monomer. Via addition of a source term van Embden et al.[22] made the seeding of an initial distribution redundant and could faithfully model the complete process of nucleation and growth over relevant time scales (Figure 2). Alternatively, Rempel et al.[23] developed a model based on kinetic rate equations (KREs) that tracks the concentration of all clusters throughout synthesis. The model is nondimensional, relying only on two scaled growth and dissociation parameters to describe NC formation and provides insight into how synthetic parameters such as additives and temperature affect the size distribution. Additionally, the authors showed that size focusing is possible in a purely reaction-limited regime (Figure 2). In a more recent study Vetter et al.[27] demonstrated that PBE and KRE methods yield similar results, while noting that KRE models potentially provide a deeper insight into the formation mechanism especially at early times, due to a superior description of subcritical clusters during nucleation. Additionally, KRE-based models can be directly extended to describe agglomeration of subcritical nuclei.[28]

To further improve existing theories it is important to subject them to quantitative evaluation and test underlying assumptions. In this regard, microfluidic reactor technology can play a significant role, through the ability to access fast kinetics as well as quantitative information on how synthetic parameters affect the resulting particles.

4. *IN SITU* SPECTROSCOPIC CHARACTERIZATION

In situ spectroscopic techniques can elucidate reaction mechanisms governing nucleation and growth, since they access information on both short and long time scales without interfering with the reaction under study.[14] *In situ* fluorescence spectroscopy is especially powerful in assaying compound semiconductor NCs, since the average size and size distribution of the synthesized NCs can be extracted from the peak wavelength and the full width at half-maximum (fwhm) of the band edge emission.[10,14] In situ fluorescence/absorbance detection can be achieved using dip probes in flask reactors;[29] however issues related to poor precursor mixing and temperature heterogeneities within the reactor volume, almost always lead to uncertainties in mechanistic studies at early time scales.

In this regard, Chan et al.[30] first presented the incorporation of a fluorescence detector with a chip-based microfluidic reactor for the analysis of CdSe NCs. Such a strategy has since been incorporated within other microfluidic formats.[31,32] Subsequently, Chan et al.[33] extended the basic idea to a two-phase format eliminating residence time distributions. These early studies enabled the quantification of how reaction parameters including temperature, reaction time, and organic ligands affect mean particle size, dispersion, and concentration. The combination of microfluidics with real-time fluorescence spectroscopy has since been applied to the synthesis of a wide variety of QDs (including CdS,[34] CdSe,[33,35,36] CdSeTe,[37] PbS,[12] PbSe,[12] InP[36,38]) and the rapid screening of QD characteristics.

DOI: 10.1021/acs.accounts.7b00088
Acc. Chem. Res. 2017, 50, 1248−1257

Although the majority of research has focused on the controlled synthesis of QDs, less attention has been devoted to the quantitative analysis of nucleation and growth[36,39−41] using a combination of real-time spectroscopic methods and theoretical modeling.

An illustrative example of the utility of microfluidics with on-line detection was reported by Sounart et al.,[42] who united separate flows of cadmium and sulfur precursors in a y-mixer. Mixing by diffusion generated a supersaturated region at the boundary of the two streams (Figure 3), and subsequent formation of CdS QDs. QD emission was monitored at different positions across and along the microfluidic channel, monitoring particle growth between 400 ms and 28 s. Interestingly, the authors demonstrated close correspondence between a diffusion-limited nucleation model (with a rate-limiting final activation process) and experimental results. Although on-line photoluminescence (PL) measurements are valuable for assessing size-dependent emission characteristics they are unable to provide a quantitative understanding of the size and concentration of nuclei during the initial steps of reaction. In contrast, absorption spectroscopy generates information relating to both particle size and concentration, while also probing the limits of nucleation and growth.[39,41]

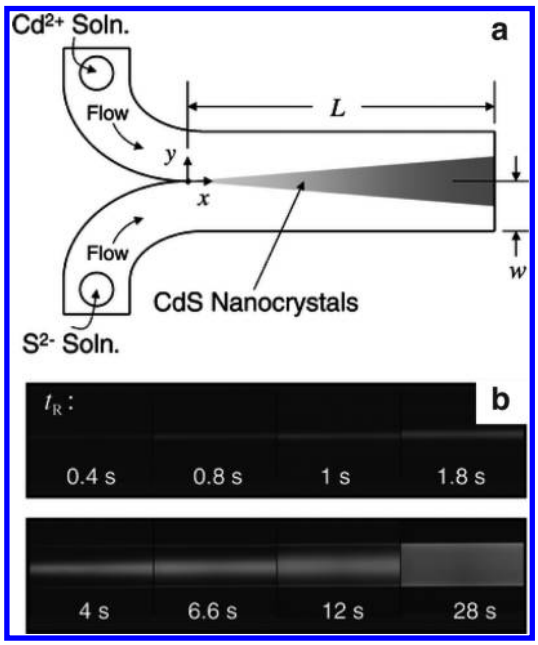

Figure 3. (a) Schematic of a continuous flow platform for injection and reaction of Cd and S precursors. (b) Time-lapse images of CdS QD fluorescence during nucleation and growth. Reprinted with permission from ref 42. Copyright 2007 Royal Society of Chemistry.

5. TUBE-BASED AUTOMATED MICROFLUIDIC REACTORS

In recent years, we have developed a family of segmented flow reactors that operate at high temperatures (up to 300 °C) and are equipped with real-time fluorescence and absorption detectors for the continuous assessment of particle characteristics. Tube-based reactors were selected over chip-based configurations due to their fabrication and operational simplicity, while offering opportunities for facile scale-out production. Such reactor configurations have proven to be robust and efficient in generating a wide variety of QDs, and we anticipate that they will be of value to the nanomaterials community at large.

5.1. Droplet Reactors: Kinetics and Synthesis

Figure 4 illustrates exemplar microfluidic and detector modules used for the synthesis of QDs. For all reactor formats, we use precision syringe pumps to motivate dispersed precursor phases and carrier fluid, which combine within standard PEEK manifolds to form nanoliter droplets. The manifolds and syringes are connected using PTFE tubing and PEEK fittings (Figure 4a). The formed droplets are subsequently directed through PTFE tubing coiled around a copper-heating rod (Figure 4b) or embedded into a heated block, which has microgrooves fabricated on its surface (Figure 4c) to allow rapid reaction initiation. To perform a two-stage reaction or preheat precursor solutions, a second heating rod or block can be added in series. The temperature is controlled within ±1 K of the set point using in-house developed controllers.

5.2. Real-Time Spectroscopic Analysis

Integrated spectroscopic systems can be categorized as on-line or in-line. On-line spectroscopic systems are able to probe reactions at several positions within the reaction zone and are suitable for quantitative assessments of fast reaction kinetics. In contrast, in-line systems enable measurements postheating and when the reaction has been quenched. The latter approach is generally convenient for monitoring of reactions with relatively slow kinetics.

Figure 4a illustrates a microfluidic setup with integrated detection modules for the simultaneous extraction of absorption and fluorescence data on millisecond to second time scales. Specifically, axial and rotational movement of the heating rod allows monitoring of the optical characteristics of QDs at different points along the reaction path. For fluorescence measurements, the collimated beam of an LED is focused into the microfluidic channel. Emission from passing droplets is analyzed spectroscopically. In contrast, absorbance detection is challenging due to limited optical pathlengths defined by the channel/capillary diameter. In addition, contained droplets will refract light propagating through them, making extraction of reference spectra difficult. To circumvent sensitivity issues, we have implemented a geometry where a sheet of light propagates in a tangential manner through the curved path of the tubing to match the length of the reaction plugs. For in-line measurements, we extract fluorescence spectra by focusing radiation of an appropriate wavelength into a translucent polymer capillary containing flowing droplets. An optical fiber connected to a spectrometer and oriented orthogonal to the incident radiation collects fluorescence (Figure 4d). For absorbance measurements, the output of a combined deuterium/halogen lamp is focused into the same capillary, with transmitted light being collected with an optical fiber (Figure 4e).

6. KINETIC STUDIES

We have demonstrated the flexibility of our platforms for the synthesis of binary, core/shell, and multinary QDs via real-time investigation of nucleation and growth kinetics. For example, we recently investigated millisecond kinetics of PbS QDs by performing both on-line absorption (Figure 5a) and PL measurements (Figure 5b) at high temperatures (>100 °C).[39] This platform enabled the synthesis of high-quality PbS QDs, while also providing real-time estimation of particle size and concentration. The limits of nucleation and growth time scales

DOI: 10.1021/acs.accounts.7b00088
Acc. Chem. Res. 2017, 50, 1248−1257

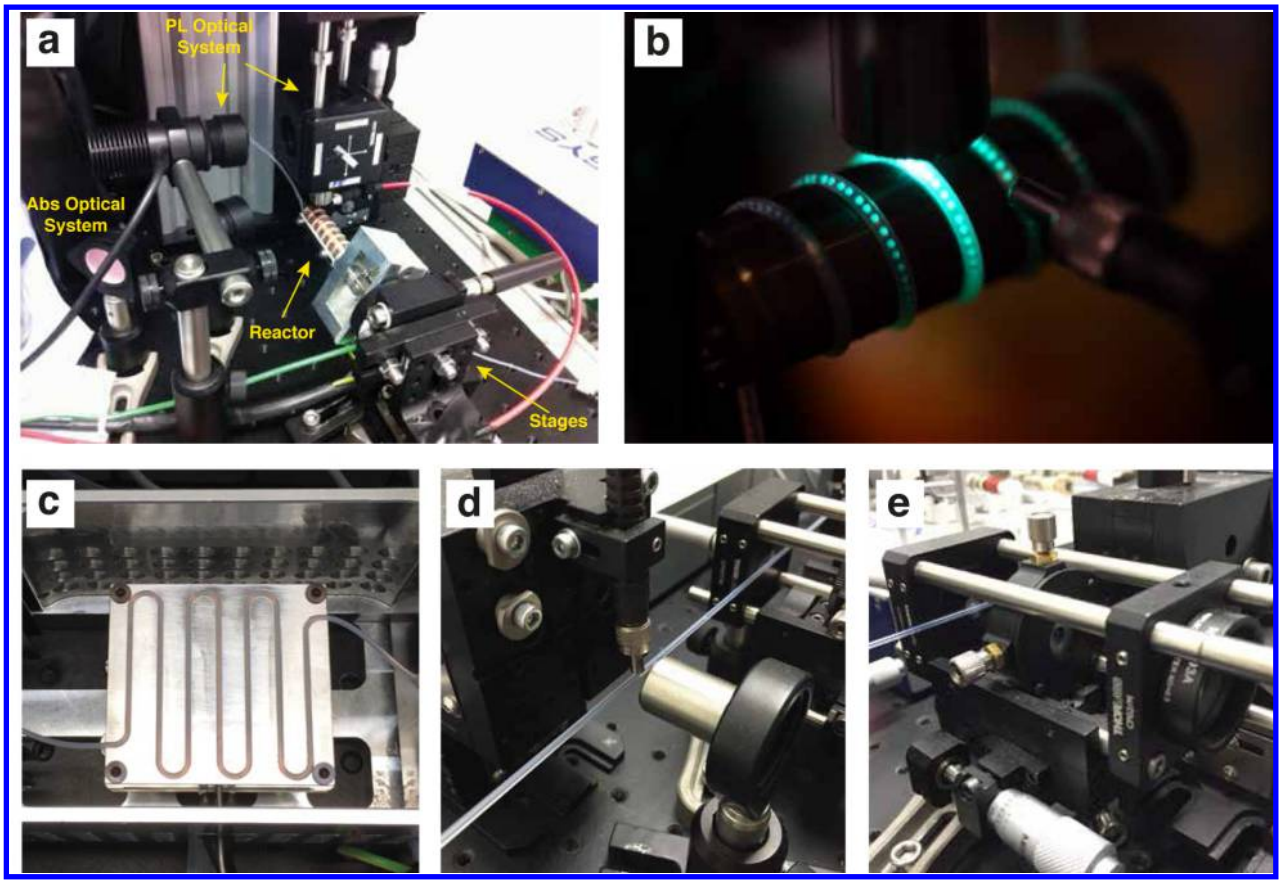

Figure 4. (a) Image of a microfluidic platform incorporating on-line absorbance and PL modules. (b) Close-up of a heating rod illustrating the motivation of nanoliter droplets through PTFE tubing. (c) Image of PTFE tubing embedded into a heated block. (d) Image of an in-line fluorescence detector. (e) Image of an in-line absorption unit.

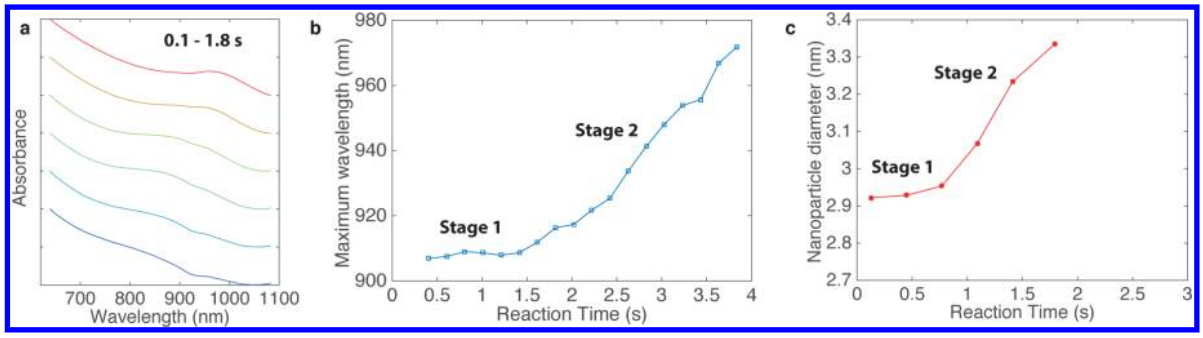

Figure 5. Investigation of nucleation and growth of PbS QDs by real-time absorption and fluorescence measurements. Temporal evolution of (a) the absorption spectra at 130 °C, (b) the position of the emission peak, and (c) the average size of PbS QDs. Reproduced with permission from ref 39. Copyright 2015 John Wiley and Sons.

were identified, revealing a two-stage reaction mechanism (Figure 5b,c). This linear growth was modeled by LSW theory indicating that Ostwald ripening is the dominant growth mechanism. Concurrent PL measurements determined the temporal evolution of the PL spectrum, which was consistent with the proposed mechanism, while also revealing a size focusing and broadening of the particle size distribution.

In a more recent study, we studied the formation of cesium lead halide perovskites.[40] Significantly, we demonstrated the rapid optimization of reaction conditions, while providing novel insights into the early stage formation and kinetics of halide perovskites, which are too fast to be effectively observed in batch reactors (Figure 6a,b). Interestingly, the temporal evolution of PL spectra obtained from mixed-halide perovskites, revealed a peculiar mechanism of either aggregation of ternary halides or inter-NC anion exchange, suggesting that direct coprecipitation of all four ions does not occur (Figure 6c). The kinetic framework draws similarities with the formation of other ternary or quaternary systems such as Cu_2ZnGe_4 and $Cu_{2-x}ZnSe_yS_{1-y}$, possessing faster nucleation and growth processes. Extending our approach to core/shell systems, we realized a two-stage microfluidic reactor, allowing for the sequential addition of new reagents in a controlled manner.[43] Crucially, the platform provides independent control of each reaction step, facilitating the synthesis of core−shell, non-heavy-metal QDs ($CuInS_2$/ZnS) (Figure 7a,b). A segmented

DOI: 10.1021/acs.accounts.7b00088
Acc. Chem. Res. 2017, 50, 1248−1257

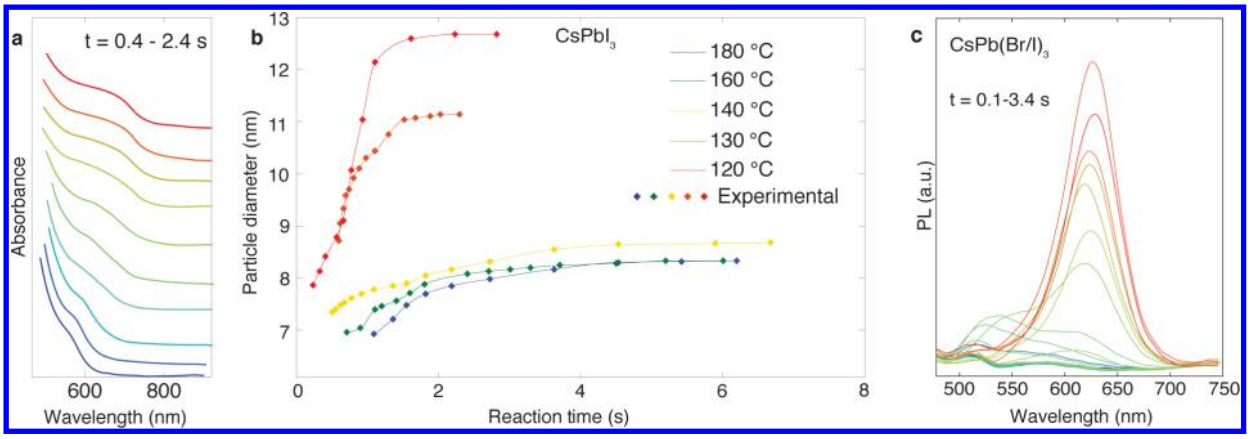

Figure 6. Investigation of the early time kinetics of $CsPbI_3$ and $CsPb(Br/I)_3$ NCs using on-line fluorescence and absorption spectroscopy. Temporal evolution of (a) absorption spectra of $CsPbI_3$ at 180 °C and (b) particle size at various temperatures (120−180 °C). (c) Variation of PL spectra of $CsPb(Br/I)_3$ as a function of reaction time. Reproduced with permission from ref 40. Copyright 2016 American Chemical Society.

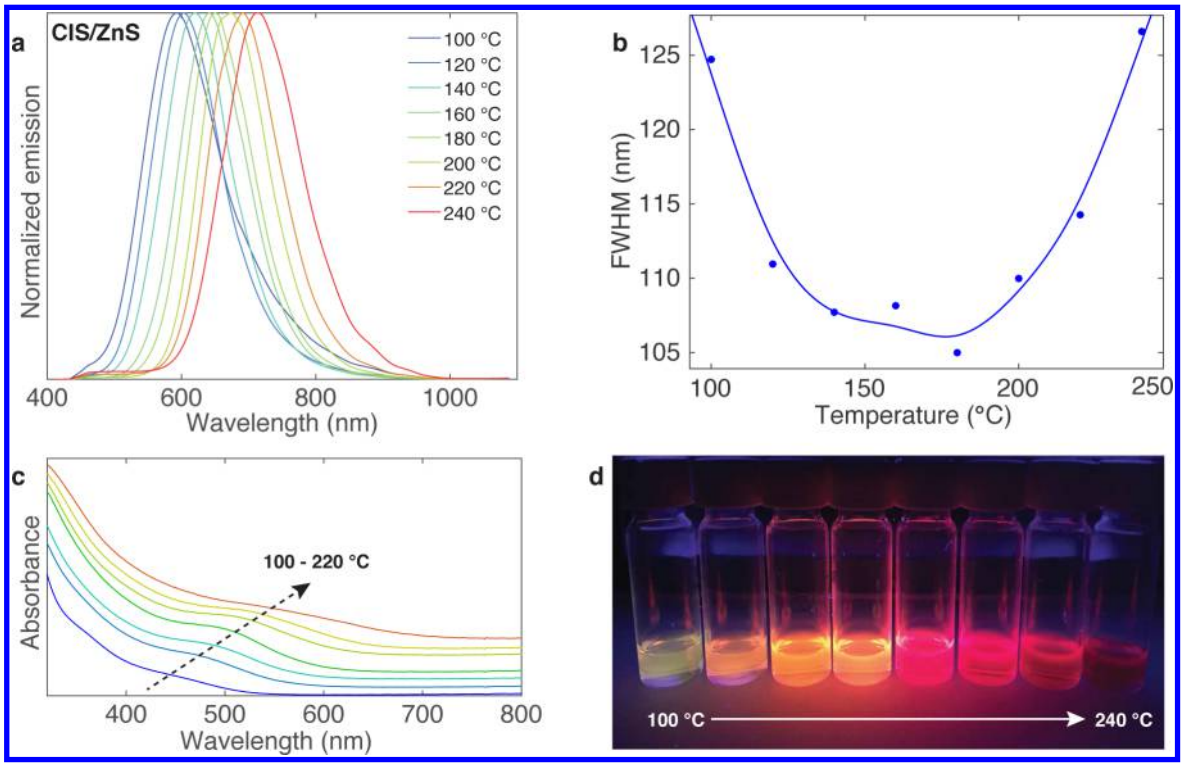

Figure 7. Effect of temperature during the formation of core NCs on (a) PL spectra, (b) fwhm of the band-edge emission, and (c) absorbance spectra of $CuInS_2$/ZnS NCs. (d) Colloidal solutions of $CuInS_2$/ZnS NCs in toluene under UV illumination (λ = 365 nm). Other parameters were Cu/In = 0.4, S/(Cu + In) = 2.65, Zn/(Cu + In) = 3, time = 32 s, and T_{shell} = 230 °C. Reprinted with permission from ref 43. Copyright 2016 Royal Society of Chemistry.

flow regime is preferred for the synthesis of $CuInS_2$ cores, with ZnS shell growth occurring in a second step. The effect of various reaction parameters such as temperature (Figure 7b,c) for $CuInS_2$ synthesis and ZnS shell growth, reaction times, and individual adjustment of Cu/In, S/(Cu + In) and Zn/(Cu + In) molar ratios, could be optimized during the synthesis of size-tunable and photostable $CuInS_2$/ZnS NCs.

As previously outlined, there are numerous theories describing NC nucleation and growth, which qualitatively agree with experimental results but lack quantitative rigor. Realizing this, we designed a fully automated two-stage microfluidic reactor equipped with fluorescence and absorbance detection after each stage (Figure 8a).[41] Experiments demonstrated that size tuning solely by variation of the reaction time and temperature does not yield particles of optimal size dispersion or yield, as predicted by theory. Rather, addition of precise amounts of precursor in conjunction with control of the reaction temperature in the second stage led to NCs of optimal yield, fwhm, and emission maximum. To gain further insight into nucleation and growth, we adopted the kinetic model developed by Rempel et al.[23] and reformulated the equations in a dimensional form to allow for direct fitting of model to experiment. Via determination of rate constants we were able to extract activation energies and model temperature dependencies. Interestingly, we observed excellent agreement between prediction and experiment for temperatures between

DOI: 10.1021/acs.accounts.7b00088
Acc. Chem. Res. 2017, 50, 1248−1257

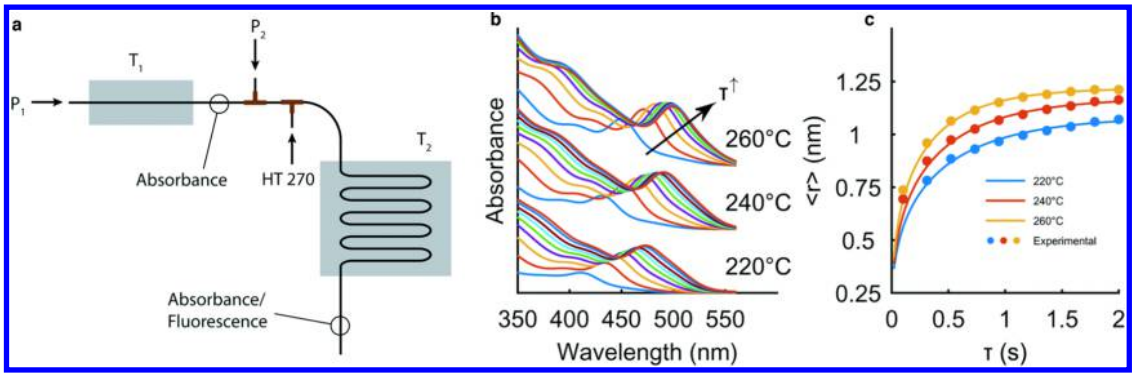

Figure 8. (a) Schematic of a two-stage microfluidic reactor with in-line absorbance and fluorescence detectors. (b) Variation of absorption spectra of CdSe QDs as a function of temperature (220−260 °C). (c) Temporal evolution of the extracted particle radius. Solid lines represent model fits. Reproduced with permission from ref 41. Copyright 2016 Royal Society of Chemistry.

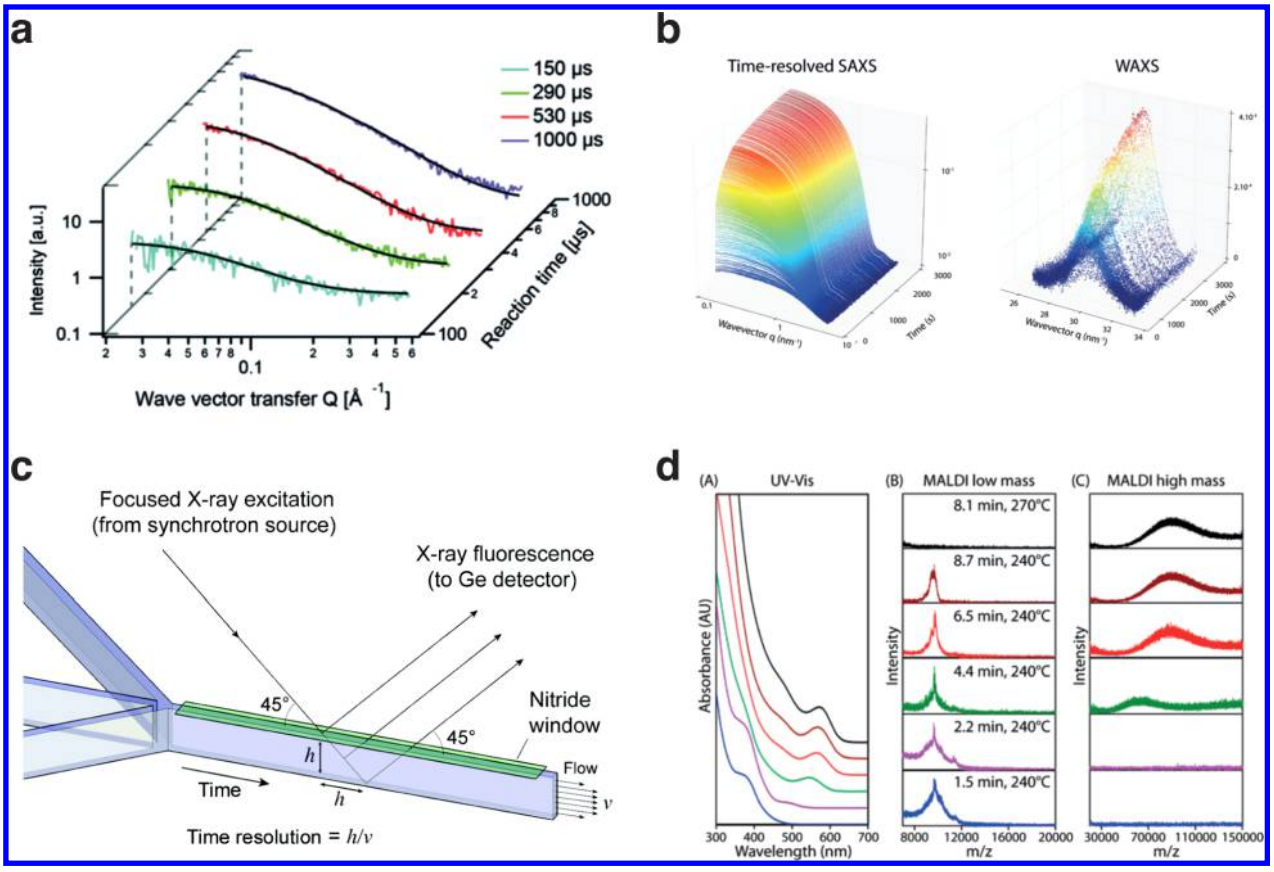

Figure 9. Structural and elemental analysis of nanomaterials. (a) Time-resolved SAXS measurements probing nucleation and growth of CdS QDs. Reprinted with permission from ref 45. Copyright 2015 Royal Society of Chemistry. (b) *In situ* synchrontron SAXS and WAXS measurements monitoring the formation of CdSe QDs. Reprinted with permission from ref 46. Copyright 2015 American Chemical Society. (c) Schematic of a continuous flow reactor incorporating real-time μXAS for the assessment of cation exchange. Reprinted with permission from ref 47. Copyright 2007 American Chemical Society. (d) UV−vis absorbance measurements and MALDI-TOF MS characterization of InP QDs synthesized in a microfluidic reactor. Reprinted with permission from ref 48. Copyright 2016 American Chemical Society.

200 and 290 °C (Figure 8b,c). It should be noted that we did not evaluate how well the model predicts the particle size distribution since we were unable to directly extract this information from spectra. Indeed, further refinement of the model will need to address this limitation.

7. COMPOSITIONAL AND STRUCTURAL CHARACTERIZATION

Fluorescence and absorption spectroscopy provide somewhat limited information regarding shape and structural characteristics, and thus alternative detection methodologies are required. In this regard, small-angle X-ray scattering (SAXS) and wide-angle X-ray scattering (WAXS) are well suited for probing such features.[44]

The combination of *in situ* SAXS with continuous flow was first demonstrated by Polte et al.[49] for the synthesis of gold NCs. Subsequently, Schiener et al.[45] investigated the nucleation and growth of CdS QDs using SAXS/WAXS (Figure 9a). Notably, the setup could probe nucleation of CdS clusters and the coexistence of nucleation and growth with microsecond

DOI: 10.1021/acs.accounts.7b00088
Acc. Chem. Res. 2017, 50, 1248−1257

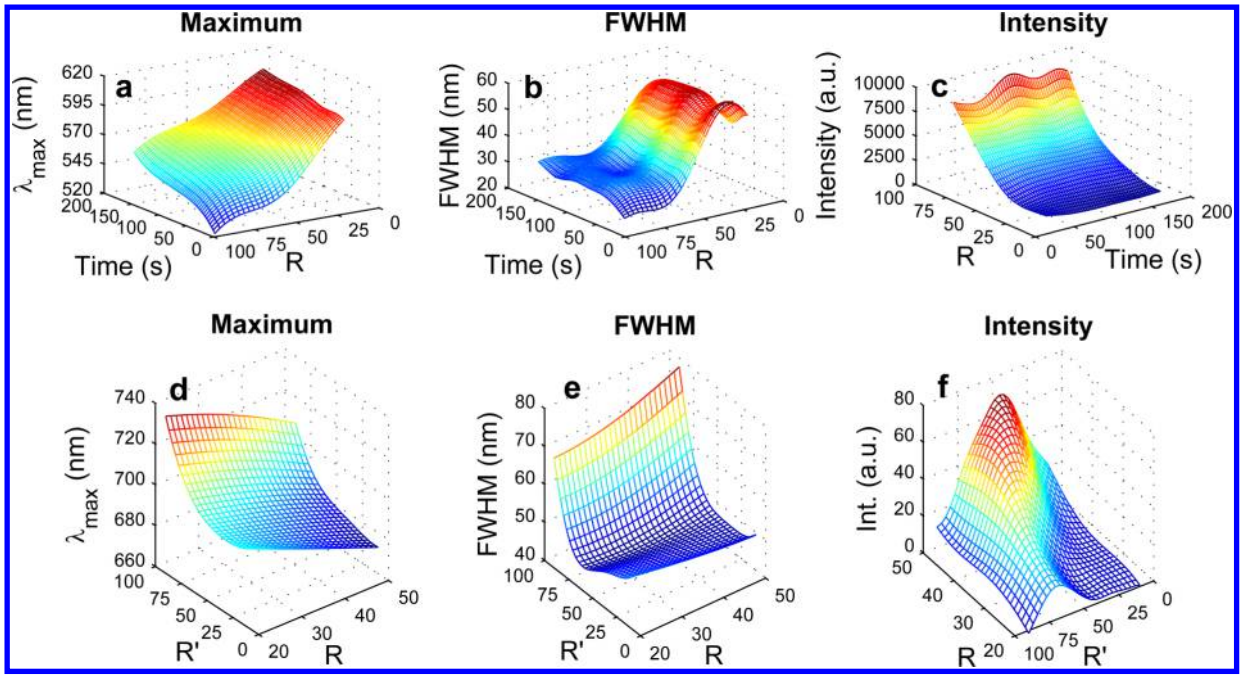

Figure 10. Optimization of synthetic parameters in the synthesis of CdSe and CdSeTe QDs. Kriging metamodels of fluorescence maximum, fwhm, and intensity for (a−c) CdSe QDs and (d−f) CdSeTe QDs. Reproduced with permission from ref 37. Copyright 2014 American Chemical Society.

resolution. In a different manner, Abécassis et al.[46] coupled a glass capillary device with time-resolved SAXS/WAXS to monitor the size evolution of CdSe QDs. Critically, parameters such as particle radius, concentration, sample dispersity, and reaction yield could be monitored with precision (Figure 9b). WAXS measurements determined a zinc blende structure of CdSe QDs, with expansion of their crystalline lattice with growth.

Chan et al.[47] used X-ray absorption spectroscopy (XAS) to investigate cation exchange between CdSe and Ag_2Se QDs in continuous flow (Figure 9c). Monitoring kinetics and structural evolution of CdSe to Ag_2Se (4−100 ms) provided detailed characterization of the reaction. However, detailed structural information on intermediate states was inaccessible without incorporation of EXAFS (extended X-ray absorption fine structure) measurements. In a similar vein Uehara et al.[50] reported an EXAFS analysis of nucleation during the synthesis of CdSe QDs, which indicated a rapid initial increase in CdSe nuclei concentration along with a concomitant decrease during growth.

Recently, Xie et al.[48] used a flow reactor and matrix-assisted laser desorption/ionization time-of-flight (MALDI-TOF) mass spectrometry (MS) to study the growth mechanisms of InP QDs. Building upon recent innovations in continuous particle purification using gel permeation chromatography,[51] the authors demonstrated the synthesis and continuous purification of InP QDs in air-free conditions. MALDI-TOF MS revealed the existence of InP clusters during particle growth that act as stock for the production of QDs (Figure 9 d). A deeper understanding of growth mechanisms led to a predictive design of cluster-free InP QDs and allowed for the quantization of extinction coefficients and generation of size curves. To this end, we believe that the integration of continuous purification and *in situ* elemental analysis with microfluidics could provide unprecedented control over the purity of QDs, while facilitating the investigation of rapid kinetics.

8. REACTION OPTIMIZATION IN FLOW

The combination of configurable microfluidic reactors with real-time monitoring methods enables the facile implementation of optimization algorithms. We first demonstrated this concept for the synthesis of CdSe QDs by feeding steady-state fluorescence data acquired from an automated microfluidic reactor to a control algorithm.[52] Reduction of extracted data to a dissatisfaction coefficient (defining "reaction success") and incorporation of a stable noisy optimization by branch and fit (SNOBFIT) algorithm, was used to generate QDs of "optimal" properties. However, the translation of product specifications to an objective function via weighting coefficients can lead to the exclusion of desirable synthesis conditions.[52] Additionally, the "black-box" character of optimization algorithms prevents a quantitative understanding of how synthetic parameters influence product. To mitigate these problems, we recently used a Kriging metamodeling algorithm to optimize synthetic parameters used in the formation of CdSe and CdSeTe QDs.[37] Such an algorithm was able to map and reconstruct multidimensional parameter space using only a few *a priori* sampled parameters (Figure 10). Subsequently, extracted fwhm, maxima, and intensity data were used to fit a Universal Kriging metamodel. The accuracy of the approximation was remarkable considering the sparse sampling performed. Such an approach is efficient in the fast optimization of reaction parameters.

Another interesting approach was presented by Orimoto et al.,[53] who demonstrated the combinatorial synthesis of CdSe QDs in a microfluidic reactor and the use of artificial neural networks to predict reaction outcomes. This approach enabled the control and optimization of key reaction parameters, with the constructed neural networks predicting particle properties with good accuracy. It is however noted that construction of neural networks is time-consuming (2.5−5 h) and the algorithm computationally expensive.

We are certain that by unveiling reaction parameters such as rate constants, production rate and reaction yield will offer

DOI: 10.1021/acs.accounts.7b00088
Acc. Chem. Res. 2017, 50, 1248−1257

exciting opportunities for the implementation of other algorithms, thus far used only for the optimization of organic reactions.[54] Such algorithms will facilitate scale-up/scale-out of reaction processes and allow the generation of bespoke materials.

9. CONCLUSIONS AND OUTLOOK

The pioneering studies discussed herein have been critical in broadening the utility of microfluidic technology in understanding mechanisms underlying QD synthesis and generating high quality particles. Developing controlled processes for the formation of QDs and implementing real-time characterization systems can lead to the development of precise synthetic methodologies for the predictive design of existing compositions and the discovery of QDs with novel stoichiometries. To satisfy the requirements of such a technological challenge, we anticipate that further research will focus on the development of faster *in situ* spectroscopic methods[55] to monitor phenomena taking place on microsecond time scales, further expansion of the gamut of structural and elemental characterization techniques, such as *in situ* TEM, the marriage of microfluidic reactors with real-time photophysical characterization techniques, such as time-correlated single photon counting, and the exploitation of novel libraries for tunable precursors,[56] which can be directly exploited using high-throughput flow reactors, and the development of efficient predictive models for the formation of more complex nanostructures.

■ AUTHOR INFORMATION

Corresponding Author

*E-mail: andrew.demello@chem.ethz.ch.

ORCID

Andrew J. deMello: 0000-0003-1943-1356

Present Address

‡Department of Chemical Engineering, Massachusetts Institute of Technology, 77 Massachusetts Avenue, Cambridge, MA 02139, U.S.A.

Notes

The authors declare no competing financial interest.

Biographies

Ioannis Lignos received a Diploma of Engineering from NTUA, Greece, an M.Sc. in Chemical and Biochemical Engineering from EPFL, Switzerland, and a Ph.D from ETH Zurich, Switzerland. He is currently an SNF postdoctoral fellow at Massachusetts Institute of Technology (MIT) working on the synthesis of nontoxic semiconductor nanocrystals and single-dot spectroscopy.

Richard Maceiczyk received a B.Sc. in Chemistry from Heidelberg University, an M.Sc. from ETH Zurich and Nagoya University, and a Ph.D from ETH Zurich, Switzerland. He is currently working as a postdoctoral researcher at ETH Zurich where his research interests focus on the synthesis and spectroscopic analysis of nanomaterials in microfluidic systems.

Andrew J. deMello received a B.Sc. in Chemistry and a Ph.D. in Molecular Photophysics from Imperial College London. He is currently Professor of Biochemical Engineering at the Swiss Federal Institute of Technology (ETH Zurich) where his research activities focus on the development and application of microfluidic technologies in the chemical and biological sciences.

■ REFERENCES

(1) Kovalenko, M. V.; Manna, L.; Cabot, A.; Hens, Z.; Talapin, D. V.; Kagan, C. R.; Klimov, V. I.; Rogach, A. L.; Reiss, P.; Milliron, D. J.; Guyot-Sionnnest, P.; Konstantatos, G.; Parak, W. J.; Hyeon, T.; Korgel, B. A.; Murray, C. B.; Heiss, W. Prospects of Nanoscience with Nanocrystals. *ACS Nano* **2015**, *9*, 1012−1057.

(2) Thanh, N. T. K.; Maclean, N.; Mahiddine, S. Mechanisms of Nucleation and Growth of Nanoparticles in Solution. *Chem. Rev.* **2014**, *114*, 7610−7630.

(3) van Embden, J.; Chesman, A. S. R.; Jasieniak, J. J. The Heat-Up Synthesis of Colloidal Nanocrystals. *Chem. Mater.* **2015**, *27*, 2246−2285.

(4) Reiss, P.; Carrière, M.; Lincheneau, C.; Vaure, L.; Tamang, S. Synthesis of Semiconductor Nanocrystals, Focusing on Nontoxic and Earth-Abundant Materials. *Chem. Rev.* **2016**, *116*, 10731−10819.

(5) Wang, X.; Sun, G.; Li, N.; Chen, P. Quantum dots derived from two-dimensional materials and their applications for catalysis and energy. *Chem. Soc. Rev.* **2016**, *45*, 2239−2262.

(6) Howes, P. D.; Chandrawati, R.; Stevens, M. M. Colloidal nanoparticles as advanced biological sensors. *Science* **2014**, *346*, 1247390.

(7) Kagan, C. R.; Lifshitz, E.; Sargent, E. H.; Talapin, D. V. Building devices from colloidal quantum dots. *Science* **2016**, *353*, aac5523.

(8) Kovalenko, M. V. Opportunities and challenges for quantum dot photovoltaics. *Nat. Nanotechnol.* **2015**, *10*, 994−997.

(9) Lee, J.; Yang, J.; Hyeon, T.; Kwon, S. G. Nonclassical Nucleation and Growth of Inorganic Nanoparticle. *Nat. Rev. Mater.* **2016**, *1*, 16034.

(10) Phillips, T. W.; Lignos, I. G.; Maceiczyk, R. M.; deMello, A. J.; deMello, J. C. Nanocrystal synthesis in microfluidic reactors: where next? *Lab Chip* **2014**, *14*, 3172−3180.

(11) Jensen, K. F.; Reizman, B. J.; Newman, S. G. Tools for chemical synthesis in microsystems. *Lab Chip* **2014**, *14*, 3206−3212.

(12) Lignos, I.; Protesescu, L.; Stavrakis, S.; Piveteau, L.; Speirs, M. J.; Loi, M. A.; Kovalenko, M. V.; deMello, A. J. Facile Droplet-based Microfluidic Synthesis of Monodisperse IV-VI Semiconductor Nanocrystals with Coupled In-Line NIR Fluorescence Detection. *Chem. Mater.* **2014**, *26*, 2975−2982.

(13) Yen, B. K. H.; Günther, A.; Schmidt, M. A.; Jensen, K. F.; Bawendi, M. G. A Microfab- ricated Gas-Liquid Segmented Flow Reactor for High-Temperature Synthesis: The Case of CdSe Quantum Dots. *Angew. Chem., Int. Ed.* **2005**, *44*, 5447−5451.

(14) Maceiczyk, R. M.; Lignos, I. G.; deMello, A. J. Online detection and automation methods in microfluidic nanomaterial synthesis. *Curr. Opin. Chem. Eng.* **2015**, *8*, 29−35.

(15) Erdemir, D.; Lee, A. Y.; Myerson, A. S. Nucleation of Crystals from Solution: Classical and Two-Step Models. *Acc. Chem. Res.* **2009**, *42*, 621−629.

(16) Reiss, H. The Growth of Uniform Colloidal Dispersions. *J. Chem. Phys.* **1951**, *19*, 482−487.

(17) Wagner, C. Theorie der Alterung von Niederschlägen durch Umlösen (Ostwald-Reifung). *Ber. Bunsenges. Phys. Chem.* **1961**, *65*, 581−591.

(18) Lifshitz, I. M.; Slyozov, V. V. The Kinetics of Precipitation from Supersaturated Solid Solutions. *J. Phys. Chem. Solids* **1961**, *19*, 35−50.

(19) Becker, R.; Döring, W. Kinetische Behandlung der Keimbildung in übersättigten Dämpfen. *Ann. Phys.* **1935**, *416*, 719−752.

(20) LaMer, V. K.; Dinegar, R. H. Theory, Production and Mechanism of Formation of Monodispersed Hydrosols. *J. Am. Chem. Soc.* **1950**, *72*, 4847−4854.

(21) Talapin, D. V.; Rogach, A. L.; Haase, M.; Weller, H. Evolution of an Ensemble of Nanoparticles in a Colloidal Solution: Theoretical Study. *J. Phys. Chem. B* **2001**, *105*, 12278−12285.

(22) van Embden, J.; Sader, J. E.; Davidson, M.; Mulvaney, P. Evolution of Colloidal Nanocrystals: Theory and Modeling of their Nucleation and Growth. *J. Phys. Chem. C* **2009**, *113*, 16342−16355.

(23) Rempel, J. Y.; Bawendi, M. G.; Jensen, K. F. Insights into the Kinetics of Semiconductor Nanocrystal Nucleation and Growth. *J. Am. Chem. Soc.* **2009**, *131*, 4479−4489.

DOI: 10.1021/acs.accounts.7b00088
Acc. Chem. Res. 2017, 50, 1248−1257

(24) Rogach, A. L.; Talapin, D. V.; Shevchenko, E. V.; Kornowski, A.; Haase, M.; Weller, H. Organization of Matter on Different Size Scales: Monodisperse Nanocrystals and Their Superstructures. *Adv. Funct. Mater.* **2002**, *12*, 653−664.
(25) Mantzaris, N. V. Liquid-Phase Synthesis of Nanoparticles: Particle Size Distribution Dynamics and Control. *Chem. Eng. Sci.* **2005**, *60*, 4749−4770.
(26) Robb, D. T.; Privman, V. Model of Nanocrystal Formation in Solution by Burst Nucleation and Diffusional Growth. *Langmuir* **2008**, *24*, 26−35.
(27) Vetter, T.; Iggland, M.; Ochsenbein, D. R.; Hänseler, M.; Mazzotti, M. Flurin ADN Mazzotti Modeling Nucleation, Growth, and Ostwald Ripening in Crystallization Processes: A Comparison between Population Balance and Kinetic Rate Equation. *Cryst. Growth Des.* **2013**, *13*, 4890−4905.
(28) Cossairt, B. M. Shining Light on Indium Phosphide Quantum Dots: Understanding the Interplay among Precursor Conversion, Nucleation, and Growth. *Chem. Mater.* **2016**, *28*, 7181.
(29) Qu, L.; Yu, W. W.; Peng, X. In Situ Observation of the Nucleation and Growth of CdSe Nanocrystals. *Nano Lett.* **2004**, *4*, 465−469.
(30) Chan, E. M.; Mathies, R. A.; Alivisatos, A. P. Size-Controlled Growth of CdSe Nanocrystals in Microfluidic Reactors. *Nano Lett.* **2003**, *3*, 199−201.
(31) Krishnadasan, S.; Tovilla, J.; Vilar, R.; deMello, A. J.; deMello, J. C. On-line analysis of CdSe nanoparticle formation in a continuous flow chip-based microreactor. *J. Mater. Chem.* **2004**, *14*, 2655.
(32) Nakamura, H.; Tashiro, A.; Yamaguchi, Y.; Miyazaki, M.; Watari, T.; Shimizu, H.; Maeda, H. Application of a microfluidic reaction system for CdSe nanocrystal preparation: their growth kinetics and photoluminescence analysis. *Lab Chip* **2004**, *4*, 237−240.
(33) Chan, E. M.; Alivisatos, A. P.; Mathies, R. A. High-Temperature Microfluidic Synthesis of CdSe Nanocrystals in Nanoliter Droplets. *J. Am. Chem. Soc.* **2005**, *127*, 13854−13861.
(34) Edel, J. B.; Fortt, R.; deMello, J. C.; deMello, A. J. Microfluidic routes to the controlled production of nanoparticles. *Chem. Commun.* **2002**, 1136−1137.
(35) Nightingale, A. M.; Krishnadasan, S. H.; Berhanu, D.; Niu, X.; Drury, C.; McIntyre, R.; Valsami-Jones, E.; deMello, J. C. A stable droplet reactor for high temperature nanocrystal synthesis. *Lab Chip* **2011**, *11*, 1221−1227.
(36) Abolhasani, M.; Coley, C. W.; Xie, L.; Chen, O.; Bawendi, M. G.; Jensen, K. F. Oscillatory Microprocessor for Growth and in Situ Characterization of Semiconductor Nanocrystals. *Chem. Mater.* **2015**, *27*, 6131−6138.
(37) Maceiczyk, R. M.; deMello, A. J. Fast and Reliable Metamodeling of Complex Reaction Spaces Using Universal Kriging. *J. Phys. Chem. C* **2014**, *118*, 20026−20033.
(38) Baek, J.; Allen, P. M.; Bawendi, M. G.; Jensen, K. F. Investigation of Indium Phosphide Nanocrystal Synthesis Using a High-Temperature and High-Pressure Continuous Flow Microreactor. *Angew. Chem., Int. Ed.* **2011**, *50*, 627−630.
(39) Lignos, I.; Stavrakis, S.; Kilaj, A.; deMello, A. J. Millisecond-Timescale Monitoring of PbS Nanoparticle Nucleation and Growth Using Droplet-Based Microfluidics. *Small* **2015**, *11*, 4009−4017.
(40) Lignos, I.; Stavrakis, S.; Nedelcu, G.; Protesescu, L.; deMello, A. J.; Kovalenko, M. V. Synthesis of Cesium Lead Halide Perovskite Nanocrystals in a Droplet-Based Microfluidic Platform: Fast Parametric Space Mapping. *Nano Lett.* **2016**, *16*, 1869−1877.
(41) Maceiczyk, R. M.; Bezinge, L.; deMello, A. J. Kinetics of nanocrystal synthesis in a microfluidic reactor: theory and experiment. *React. Chem. Eng.* **2016**, *1*, 261−271.
(42) Sounart, T. L.; Safier, P. A.; Voigt, J. A.; Hoyt, J.; Tallant, D. R.; Matzke, C. M.; Michalske, T. A. Spatially-resolved analysis of nanoparticle nucleation and growth in a microfluidic reactor. *Lab Chip* **2007**, *7*, 908−915.
(43) Yashina, A.; Lignos, I.; Stavrakis, S.; Choo, J.; deMello, A. J. Scalable production of CuInS2/ZnS quantum dots in a two-step droplet-based microfluidic platform. *J. Mater. Chem. C* **2016**, *4*, 6401−6408.
(44) Li, T.; Senesi, A. J.; Lee, B. Small Angle X-ray Scattering for Nanoparticle Research. *Chem. Rev.* **2016**, *116*, 11128−11180.
(45) Schiener, A.; Magerl, A.; Krach, A.; Seifert, S.; Steinrück, H. G.; Zagorac, J.; Zahn, D.; Weihrich, R. In situ investigation of two-step nucleation and growth of CdS nanoparticles from solution. *Nanoscale* **2015**, *7*, 11328−11333.
(46) Abécassis, B.; Bouet, C.; Garnero, C.; Constantin, D.; Lequeux, N.; Ithurria, S.; Dubertret, B.; Pauw, B. R.; Pontoni, D. Real-Time in Situ Probing of High-Temperature Quantum Dots Solution Synthesis. *Nano Lett.* **2015**, *15*, 2620−2626.
(47) Chan, E. M.; Marcus, M. A.; Fakra, S.; ElNaggar, M.; Mathies, R. A.; Alivisatos, A. P. Millisecond Kinetics of Nanocrystal Cation Exchange Using Microfluidic X-ray Absorption Spectroscopy. *J. Phys. Chem. A* **2007**, *111*, 12210−12215.
(48) Xie, L.; Shen, Y.; Franke, D.; Sebastian, V.; Bawendi, M. G.; Jensen, K. F. Characterization of Indium Phosphide Quantum Dot Growth Intermediates Using MALDI-TOF Mass Spectrometry. *J. Am. Chem. Soc.* **2016**, *138*, 13469−13472.
(49) Polte, J.; Erler, R.; Thünemann, A. F.; Sokolov, S.; Ahner, T. T.; Rademann, K.; Emmerling, F.; Kraehnert, R. Nucleation and growth of gold nanoparticles studied via in situ small angle X-ray scattering at millisecond time resolution. *ACS Nano* **2010**, *4*, 1076−1082.
(50) Uehara, M.; Sun, Z. H.; Oyanagi, H.; Yamashita, K.; Fukano, A.; Nakamura, H.; Maeda, H. In situ extended x-ray absorption fine structure study of initial processes in CdSe nanocrystals formation using a microreactor. *Appl. Phys. Lett.* **2009**, *94*, 063104.
(51) Shen, Y.; Roberge, A.; Tan, R.; Gee, M. Y.; Gary, D. C.; Huang, Y.; Blom, D. A.; Benicewicz, B. C.; Cossairt, B. M.; Greytak, A. B. Gel permeation chromatography as a multifunctional processor for nanocrystal purification and on-column ligand exchange chemistry. *Chem. Sci.* **2016**, *7*, 5671−5679.
(52) Krishnadasan, S.; Brown, R.; deMello, A.; deMello, J. Intelligent routes to the controlled synthesis of nanoparticles. *Lab Chip* **2007**, *7*, 1434.
(53) Orimoto, Y.; Watanabe, K.; Yamashita, K.; Uehara, M.; Nakamura, H.; Furuya, T.; Maeda, H. Application of Artificial Neural Networks to Rapid Data Analysis in Combinatorial Nanoparticle Syntheses. *J. Phys. Chem. C* **2012**, *116*, 17885−17896.
(54) Reizman, B. J.; Jensen, K. F. Feedback in Flow for Accelerated Reaction Development. *Acc. Chem. Res.* **2016**, *49*, 1786−1796.
(55) Maceiczyk, R.; Shimizu, H.; Müller, D.; Kitamori, T.; deMello, A. A Photothermal Spectrometer for Fast and Background-Free Detection of Individual Nanoparticles in Flow. *Anal. Chem.* **2017**, *89*, 1994−1999.
(56) Hendricks, M. P.; Campos, M. P.; Cleveland, G. T.; Jen-La Plante, I.; Owen, J. S. A tunable library of substituted thiourea precursors to metal sulfide nanocrystals. *Science* **2015**, *348*, 1226−1230.

DOI: 10.1021/acs.accounts.7b00088
Acc. Chem. Res. 2017, 50, 1248−1257